Macromolecules
ARTICLE

Macromolecules **2009**, *42*, 9307–9311 **9307**
DOI: 10.1021/ma901975b

Thermodynamics in Conformational Transition of Poly(β-benzyl L-aspartate) As Studied by High-Resolution Solid-State ^{13}C NMR Spectroscopy

Azusa Nakanishi,[†] Akira Shoji,[‡] and K. Takegoshi*,[†]

[†]*Department of Chemistry, Graduate School of Science, Kyoto University, Kyoto 606-8502, Japan, and* [‡]*Department of Chemistry and Chemical Biology, Graduate School of Engineering, Gunma University, Gunma 376-8515, Japan*

Received September 4, 2009; Revised Manuscript Received October 9, 2009

ABSTRACT: The thermodynamic characteristics associated with conformational change of poly(β-benzyl L-aspartate) (PBLA) in the solid state are studied by using ^{13}C high-resolution solid-state NMR. PBLA was chosen because four different conformations, i.e., the right-handed (α_R-) and left-handed α-helices (α_L-helix), left-handed ω-helix (ω_L-helix), and antiparallel β-sheet (β-sheet), can be prepared separately, and the thermally induced transition occurs among them. In this work, we analyze spectral changes due to conformational transformation of PBLA and determine the enthalpic and entropic changes associated with the transformation of α_R-helix to other conformations; the enthalpic change ΔH per residue becomes ca. 1.4 kJ mol^{-1}, and the entropic change ΔS per residue becomes ca. 3.5 J K^{-1} mol^{-1}. With using these ΔH and ΔS values, we show that the observed transition curve can be reproduced by a simple statistical model.

1. Introduction

A mechanism that leads a polypeptide to fold into a particular secondary structure is a topic of long-standing interest. To clarify the mechanism, determination of the thermodynamic parameters of secondary structures is of prime importance. For such studies, poly(β-benzyl L-aspartate) (PBLA) is a quite excellent model polypeptide because four conformations, i.e., the right-handed (α_R-) and left-handed α-helices (α_L-helix),[1] left-handed ω-helix (ω_L-helix),[2] and antiparallel β-sheet (β-sheet),[3] can be prepared by precipitation from the concentrated chloroform solution or by treating with temperature. Previous studies have reported the conditions that affect the conformational stability of PBLA and the transition from one conformation to another.[3,4] Recently, the conformational transformation of PBLA in the solid state has been studied with the high-resolution solid-state NMR method, and the relation between the secondary structure (main-chain conformation) of PBLA and the ^{13}C or ^{15}N NMR chemical shift parameter has been established.[5−9] However, no studies so far have been reported on thermodynamic parameters of secondary structure of polypeptides in the solid state. In this work, we present ^{13}C high-resolution solid-state NMR spectra of various heat-treated PBLA samples and analyze spectral changes due to conformational transformation of PBLA. From the analysis, we determine the enthalpic and entropic changes (ΔH and ΔS) associated with the transformation. Further, it is shown that, by using the obtained ΔH and ΔS values, a simple statistical model proposed by Zimm and Bragg[10] does reproduce the observed transition curve.

2. Experimental Section

2.1. Samples. Poly(β-benzyl L-aspartate) (PBLA-1, MW = 26 600) was purchased from Sigma Chemical Co. Ltd. Each PBLA powder sample of the weight of 20−25 mg was heated under N_2 gas in an oil bath at various controlled temperatures for various heat-treatment time. After heating, the samples were quickly quenched into icy water to freeze the conformational transition of the samples. The temperature of the oil bath was kept constant within ±2 K by a control system. Heat treatment was done at six different temperatures (378, 388, 393, 398, 403, and 408 K), which encompass the temperature of the endothermic peak observed by DSC measurement (not shown).

Four reference PBLA samples, having different dominant conformations, were prepared as follows from PBLA synthesized in our laboratory (PBLA-2). PBLA-2 was obtained by polymerization of β-benzyl L-aspartate-*N*-carboxy anhydride in 1,2-dichloroethane at 303 K using triethylamine as an initiator, as reported previously.[6] The conformation of the PBLA-2 sample thus obtained was the α_R-helix form. The α_L-helix form was obtained from the α_R-helix sample by precipitation from the concentrated chloroform solution and diethyl ether system. The α_R sample can also be converted either to the ω_L form or to the β form by heating at 423 K for 3.5 h or at 493 K for 3 h, respectively, in vacuo.[2,11]

2.2. NMR Measurements. The NMR experiments were carried out at 14 T by using an Apollo spectrometer and a triply tuned CPMAS probe (Doty Sci. Inc.) for 4 mm rotors. The resonance frequency is 150.918 MHz for ^{13}C. The observed ^1H spin−lattice relaxation times in the laboratory frame (T_1) and in the rotating frame ($T_{1\rho}$) for the α_L-helix, α_R-helix, and β-sheet samples of PBLA-2 are similar ($T_1 \sim 1.5$ s and $T_{1\rho} \sim 3.0$ ms) while those for ω_L-helix are longer ($T_1 \sim 2.0$ s and $T_{1\rho} \sim 7.0$ ms). In the following, we show that the ω_L-helix signals are not appreciable in PBLA-1. Hence, in this work, we use a contact time for CP of 2 ms and a recycling-delay time of 4 s for all samples and assume that the relative intensity of the peaks corresponding to each conformation in a ^{13}C spectrum is proportional to the amount of each conformer in the sample. The rf-field intensity for both CP and ^1H CW decoupling was about 70−80 kHz. The ^{13}C chemical shifts were calibrated in ppm relative to TMS by taking the ^{13}C chemical shift of the

*To whom correspondence should be addressed: Fax +81-75-753-4011; Tel +81-75-753-4015; e-mail takeyan@kuchem.kyoto-u.ac.jp.

Published on Web 10/19/2009

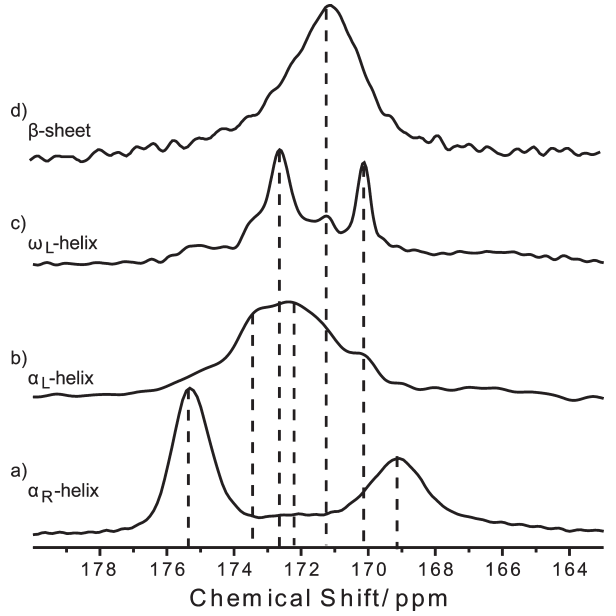

Figure 1. ^{13}C CPMAS spectra of PBLA-2, whose dominant conformation is (a) α_R, (b) α_L, (c) ω_L, and (d) β. Only the C=O region is plotted. The vertical dotted lines designate the positions of the isotropic chemical shifts listed in Table 1.

Table 1. ^{13}C Isotropic Chemical Shifts (ppm) of Carbonyl and Ester Carbons of PBLA-1 for the Four Secondary Structures

	α_R	α_L	ω_L	β
carbonyl	175.09	173.31	172.72	171.32
ester	169.16	172.29	170.15	171.32

methine carbon nuclei of solid adamantane (29.5 ppm) as an external standard. All the experiments were made at room temperature under the magic-angle spinning (MAS) frequency of 14 kHz.

3. Results and Discussion

Figure 1 shows the ^{13}C spectra of the four reference samples of PBLA-2. In Figure 1, only the C=O region is shown, which contains the signals of the carbonyl (C=O) carbon in the main chain and the ester carbon in the side chain. The measured ^{13}C isotropic chemical shifts of the two carbons in α_R, α_L, ω_L, and β forms, reported in Table 1, were used for spectral fitting. The measured values are similar to those reported previously,[5–9] but some deviations are notable, which may be attributed to the better resolution achieved by using a higher magnetic field (14 T) in this work.

Figure 2 shows spectral changes induced by increasing time of heat treatment for PBLA-1 sample at 398 K. In comparison with the spectra in Figure 1, it is clear that the structure of the commercial PBLA-1 sample without heat treatment is mostly α_R-helix (Figure 2a). With the heat treatment at 398 K for 1 min (Figure 2b), 2 min (Figure 2c), and 5 min (Figure 2d), it is notable that the intensities of the carbonyl and ester carbon signals of the α_R-helix at ca. 175 and 169 ppm, respectively, decrease with concomitant increase of resonance signals between 171 and 173 ppm. The observed spectral changes are consistent with the previously reported conformational changes, namely, α_R-helix gradually changed to β-sheet.[9]

The relative peak intensities were determined by using least-squares fitting the observed carbonyl and ester spectra to a sum of Gaussian peaks. Table 1 indicates that seven peaks may be used for fitting. In the course of analyzing the experimental data, we found that inclusion of the ω_L does not improve the fitting

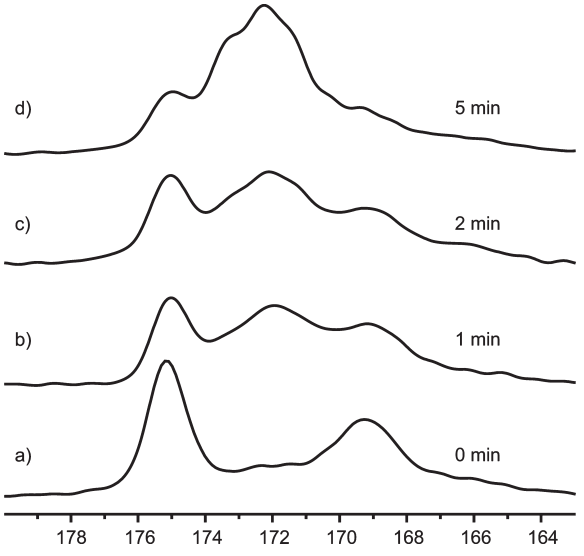

Figure 2. ^{13}C CPMAS spectra of PBLA-1 after heating at 398 K for various times.

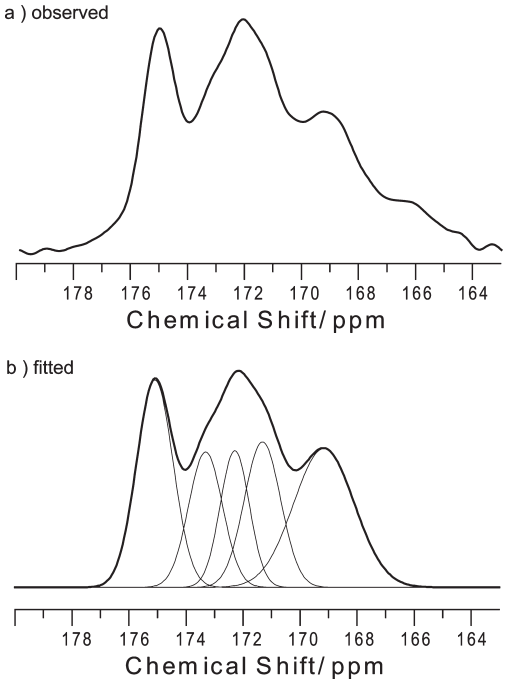

Figure 3. Signal decomposition of ^{13}C CPMAS spectrum. (a) Observed spectrum of PBLA-1 heated at 398 K for 2 min and (b) least-squared fitting of the spectrum (a) with using five Gaussian peaks.

appreciably; the relative ratios for the ω_L signals obtained are less than 2%. We therefore omitted the ω_L peaks from the spectral analysis; in other words, six peaks (five peak positions) were used for fitting. The absence of the ω_L conformation in the heat-treated PBLA-1 samples may be attributed to its structural instability for PBLA with smaller molecular weight than that of the reference PBLA-2 sample synthesized.[6]

Figure 3 shows that the observed ^{13}C spectrum of PBLA-1 heated at 398 K for 2 min (Figure 3a) can be fitted adequately to the sum of five Gaussian peaks (Figure 3b). The relative intensities of the carbonyl and the ester peaks thus obtained were added for each conformation (α_R, α_L, and β), and the fractional contents were plotted as a function of the heat-treatment time. Figure 4 shows the results for three of the six heat-treatment temperatures examined.

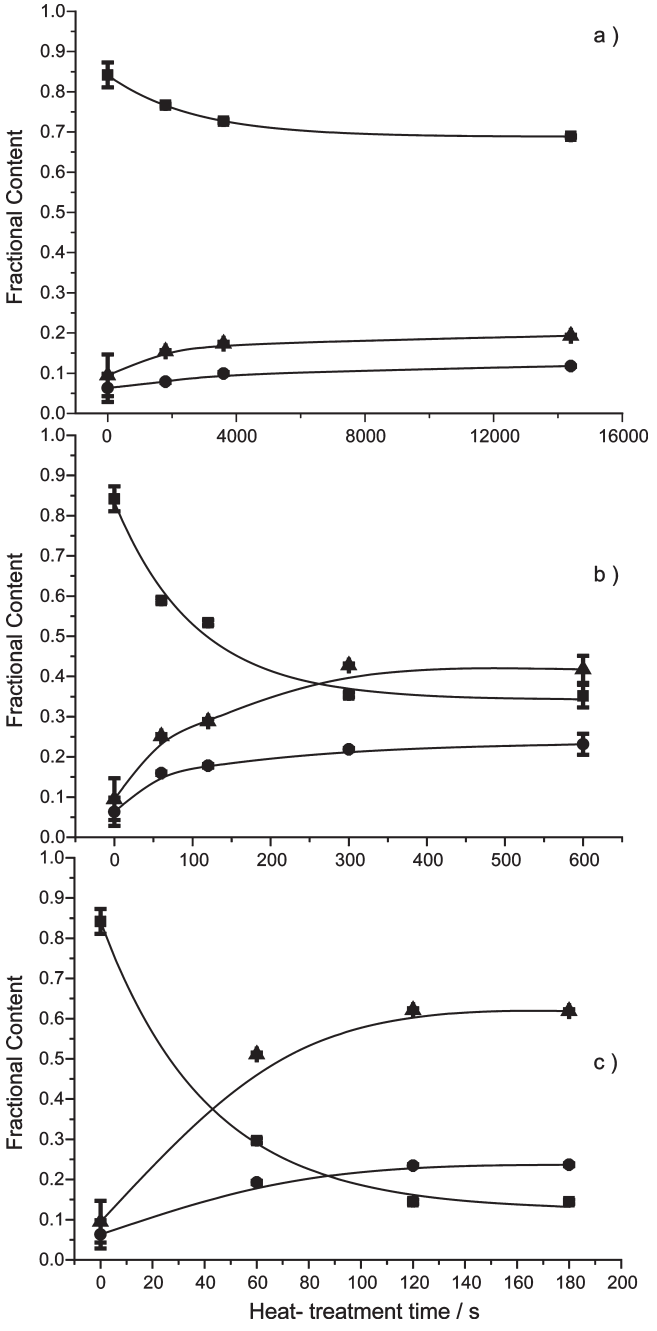

Figure 4. Fractional content of α_R (squares), α_L (triangles), and β (circles) plotted against the heat-treatment time at (a) 388, (b) 398, and (c) 408 K. The solid line for α_R (squares) is the best-fit one while the other two lines are for eye guidance.

Prior to a quantitative analysis of the results, several features may be invoked via simple inspection of the raw data in Figure 4. The postulated route for the conformational transformation upon heating,[3,9] namely, α_R, changes at first to α_L (ω_L) and finally converted into β is an oversimplified picture. Figure 4 clearly indicates that α_R changes to either α_L or β. In fact, not all α_R changes into another conformations; some α_R remains even at a longer heat-treatment time. This invokes us that at the longest heat-treatment time for each heat-treatment temperature the PBLA sample reaches a thermal equilibrium. Note here that at the lowest heat-treatment temperature (378 K) the ratios for α_L and β do not increase appreciably even with heat treatment of 4 h. Therefore, for this temperature, we did not assume that the thermal equilibrium is achieved and omitted from the following analysis.

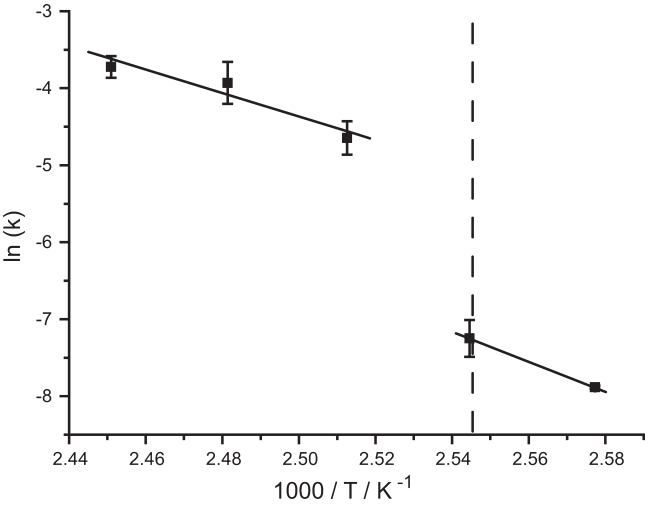

Figure 5. Rate constant k plotted against the heat-treatment temperature. The temperature of the endothermic peak observed by DSC measurement (ca. 397 K) is designated by the vertical dotted line. The solid lines are for eye guidance.

For simplicity, we express the transformation of α_R to another conformation by first-order reaction, with its rate equation given by

$$\frac{d(A(t)-A_1)}{dt} = -k(A(t)-A_1) \quad (1)$$

where $A(t)$ is the fractional content of α_R, k is the rate constant, and A_1 is the fractional content of α_R at thermal equilibrium. Equation 1 can be formally solved to as

$$A(t) = A_1 + (A_0 - A_1)\exp(-kt) \quad (2)$$

where A_0 is the fractional content of α_R at $t = 0$. By taking A_0, A_1, and k as adjustable, we least-squares fitted the observed heat-treatment time dependence of the α_R data to eq 2. The solid lines associated with the α_R data (the square) in Figure 4 are the best-fit ones. We analyzed all heat-treated spectra in a similar way to deduce A_0, A_1, and k at each heat-treatment temperature T_{HT}, and the best-fitted rate constants k were plotted against T_{HT} in Figure 5. It is clear that there is a transition of the k value between 393 and 398 K. This temperature is consistent with the temperature of the endothermic peak observed by measurement DSC (ca. 392 K; DSC data not shown).

In the above, it was indicated that the "α_R to other" transformation can be approximately expressed by using the single first-order rate equation. This leads us to estimate the conformational excess energy ΔE from A_1 at each T_{HT} by assuming the Boltzmann distribution for α_R:

$$\Delta E = -k_B T_{HT}\left(\ln \frac{1-A_1}{A_1}\right) \quad (3)$$

The obtained ΔE values are then plotted against T_{HT} in Figure 6. Interestingly, we found a linear relationship between ΔE and T_{HT}. This linearity further suggested us to express ΔE using the Gibbs free energy ΔG as

$$\Delta E = \Delta G = \Delta H - T\Delta S \quad (4)$$

where ΔH and ΔS are enthalpic and entropic changes in the conformational transformation. By fitting the observed ΔE vs T_{HT} data to eq 4, we have the best-fitted ΔH and ΔS values as

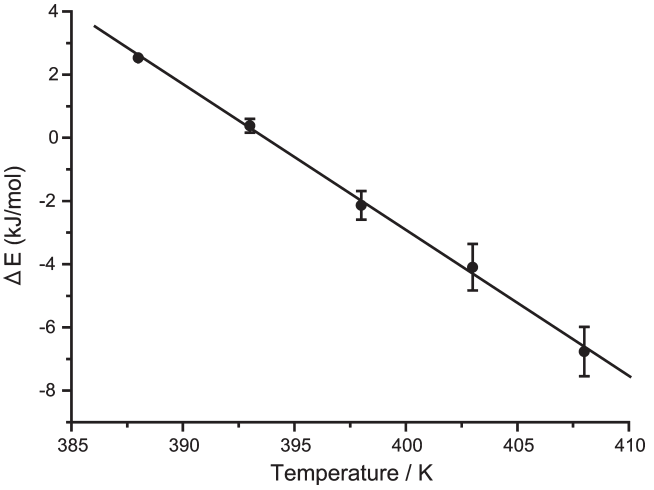

Figure 6. Transition energy plotted against heat-treatment temperature. Solid line was obtained by least-squared fitting of the experimental data to eq 4.

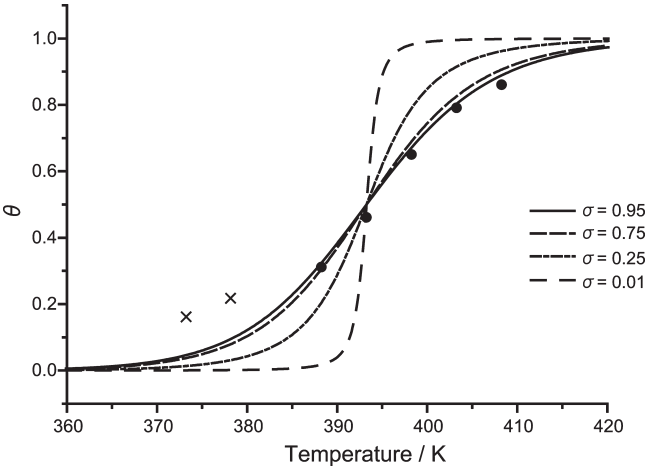

Figure 7. The relation between θ and the heat-treatment temperature; the filled circles are the experimental values, and the lines are calculated using eqs 5, 7, 12 and experimentally obtained ΔH and ΔS for five different σ values as designated in the figure. The crosses are the experimental values obtained for samples not reached to thermal equilibrium.

182 ± 5 kJ mol^{-1} and 461 ± 11 J K^{-1} mol^{-1}, respectively. The positive enthalpic change is consistent with the endothermic peak observed by DSC measurement and the positive entropic change indicates that the "α_R to other" transformation is driven by entropy. From the averaged molecular weight of PBLA-1 (MW = 26 600), we calculated the averaged number of the residues in our sample is about 130. Hence, the enthalpic change ΔH per residue becomes ca. 1.4 kJ mol^{-1} and the entropic change ΔS per residue becomes ca. 3.5 J K^{-1} mol^{-1}.

Wildman et al. examined the stability of β-sheet in poly(L-alanine) (PLA) by using solid-state NMR.[12] They analyzed ^{13}C CPMAS spectra of PLA after mechanical grinding to obtain equilibrated ratios of α-helix and β-sheet at room temperature and 77 K for two PLA samples with different molecular weight. From the two ratios, they obtained $\Delta G = -260$ J mol^{-1} for the conversion of α_R-helix to β-sheet. Hence, for both PBLA and PLA, β-sheet is more stable than α_R-helix in the solid state. As PLA does not have conformationally flexible side chain, this implies the conformational entropies of the PBLA and PLA backbones in their β-sheet conformations are larger than those in their α_R-helices. For a PLA random coil, a conformational entropy of ~14 J K^{-1} mol^{-1} per residue has been estimated[13] and, as expected, is larger than the ΔS value observed for the α_R-helix to other conformations in PBLA.

In solution, conversion of secondary structures is affected largely by environment, leading intuitive discussion of the thermodynamical parameters obtained more complex. For a recent example, Meier and Seelig examined the effect of chain length of $(KIGAKI)_n$ peptide on the conformational change from a random coil conformation to a β-sheet structure in a membrane environment.[14] They found a negative free folding energy of $\Delta G = -630$ J mol^{-1} per residue and a negative entropy term $T\Delta S = -0.4$ to -2.1 kJ mol^{-1} per residue; the reaction is endothermic and is driven by entropy. As the β-sheet formed on the membrane surface is a better ordered system, the positive entropy contribution deserves some explanation, which they ascribed to release of hydration water.

In Figure 7, we plot the fractional content of non-α_R conformations at equilibriumas $\theta = 1 - A_1$ as a function of T_{HT}. Further for comparison, we plot the fractional content of non-α_R conformations obtained for the lowest T_{HT} (378 K) at heat-treatment time of 4 h and that obtained for a non-heat-treatment sample (plotted at 373 K). Note that, for these two, the system is not fully equilibrated. Figure 7 is the so-called transition curve, and to explain its shape we adopted the matrix model proposed by Zimm and Bragg.[10] In this model, it is assumed that each residue of a polypeptide can adopt one of only two conformations; in the present case, PBLA was described as a sequence of the α_R-helix region and the non-α_R-helix region. Here we denote the two regions by "0" and "1", and the equilibrium constant s for the "0" to "1" transition is given by using the free energy ΔG in eq 4 as

$$s = \exp(-\Delta G/RT) \tag{5}$$

Further, we define the statistical weight g as follows: $g = 1$ for any "0" that appears (after a "0" or "1"); $g = s$ for any "1" that appears after another "1"; $g = \sigma s$ for any "1" that appears after "0". The parameter σ is introduced for the idea that there should be a difference between "1" after "0" and "1" after another "1". For most proteins, it is envisaged that $\sigma \ll 1 < s$ because the propagation of non-α_R conformation is more favorable than nucleation of non-α_R conformation from α_R conformation. Suppose the initial state of a peptide is all "0"; a small σ factor means that it is difficult to have a seed of "1". However, in the present case, σ is considered to be large because the initial nonheat treated sample already contains "1" (non-α_R conformation).

The partition function Z for the sequence that has n elements with k'1's sequence can be described as

$$Z = Z_1^n + Z_2^n \tag{6}$$

$$Z_1 = \frac{1}{2}\{1 + s + [(1-s)^2 + 4\sigma s]^{1/2}\} \tag{7}$$

and

$$Z_2 = \frac{1}{2}\{1 + s - [(1-s)^2 + 4\sigma s]^{1/2}\} \tag{8}$$

If the macromolecule has n elements, then we have

$$Z = 1 + \sum_{k=1}^{n} A_k \sigma s^k \quad (A_k = n - k + 1) \tag{9}$$

The probability $p(k)$, which means that there are k'1's, can be

calculated as

$$p(k) = \sigma s^k (n-k+1)/Z \tag{10}$$

Then the fraction of non-α_R, denoted by θ, is given by

$$\theta = \frac{\langle k \rangle}{n} = \sum \frac{kp(k)}{n} = \sum \frac{(n-k+1)k\sigma s^k}{nZ} \tag{11}$$

With $\sum k[(n-k+1)\sigma s^k] = s\mathrm{d}Z/\mathrm{d}s$, we have

$$\theta = (s/nZ)\,\mathrm{d}Z/\mathrm{d}s = (1/n)\,\mathrm{d}\log Z/\mathrm{d}\log s \tag{12}$$

Using eqs 2, 3 and 9 and the experimentally obtained ΔH and ΔS values, the relation between θ and T can be calculated for a σ value. A satisfactory agreement between the experimental and the calculated data is observed for $\sigma > 0.75$. The discrepancy at low temperatures can be ascribed to the insufficient heat treatment to achieve thermal equilibrium. The above analysis shows that the simple Zimm−Bragg model can be applied to conformational transformation occurring in the solid state.

In this work, we used the fractional content of the α_R signal for conformational analysis and determined the enthalpic and the entropic changes for the "α_R to the other" process. Similar analysis can also be applied for the other signal, say, the β signal to obtain the thermodynamical parameters for the formation of β-sheet. Since the β signal is overlapped appreciably by the α_L and ω_L signals and further the temperature range we used for heat treatment is too low to obtain intense β signals, we have not tried to analyze the β signal. Furthermore, the choice of α_L as the initial conformation would also be interesting as it allows us to study the disentanglement process of α_L. Such experiments are undergoing and will be published elsewhere.

Lastly, we would like to point out that the present work does not answer a question of whether do each of these regular PBLA conformations exist in a separate solid phase or do they simultaneously exist along each PBLA chain. Neither previous X-ray studies nor DSC measurements can clarify this so far. We are currently examining this by solid-state NMR, and the result will be published elsewhere.

Acknowledgment. This work was supported in part by Grants-in-aid for Scientific Research (A) (Grant No. 21248015 to K.T.) from the Ministry of Education, Culture, Sports, Science and Technology of the Japanese Government.

References and Notes

(1) Bradbury, E. M.; Downie, A. R.; Elliott, A.; Hanby, W. E. *Proc. R. Soc. London* **1960**, *A259*, 110–128.
(2) Bradbury, E. M.; Brown, L.; Downie, A. R.; Elliott, A.; Fraser, R. D. B.; Hanby, W. E. *J. Mol. Biol.* **1962**, *5*, 230–247.
(3) Kyotani, H.; Kanetsuna, H. *J. Polym. Sci., Part B* **1972**, *10*, 1931–1939.
(4) Kyotani, H.; Kanetsuna, H.; Oya, M. *J. Polym. Sci., Part B* **1977**, *15*, 1029–1036.
(5) Saito, H.; Tabeta, R.; Ando, I.; Ozaki, T.; Shoji, A. *Chem. Lett.* **1983**, *12*, 1437–1440.
(6) Ashikawa, M.; Shoji, A.; Ozaki, T.; Ando, I. *Macromolecules* **1999**, *32*, 2288–2292.
(7) Yamazaki, Y.; Kuroki, S.; Ando, I. *J. Mol. Sci.* **2002**, *608*, 183–191.
(8) Murata, K.; Katoh, E.; Kuroki, S.; Ando, I. *J. Mol. Struct.* **2004**, *689*, 223–235.
(9) Akieda, T.; Miura, H.; Kuroki, S.; Kurosu, H.; Ando, I. *Macromolecules* **1992**, *25*, 5794–5797.
(10) Zimm, B.; Bragg, J. *J. Chem. Phys.* **1959**, *31*, 526–535.
(11) Bradbury, E. M.; Carpenter, B. G.; Stephens, R. M. *Biopolymers* **1968**, *6*, 905–915.
(12) Wildman, K. A. H.; Lee, D. K.; Ramamoorthy, A. *Biopolymers* **2002**, *64*, 246–54.
(13) Tonelli, A. E. *Macromolecules* **1992**, *25*, 7199–7203.
(14) Meier, M.; Seelig, J. *J. Am. Chem. Soc.* **2008**, *130*, 1017–1024.